eCommons (2019) https://doi.org/10.7298/tbxj-3067

7 APPLICATIONS, ANCILLARY SYSTEMS, AND FUSION

Lead Author: Jennifer Wozencraft[a]

Contributing Authors: Lauren Dunkin[b], Eve Eisemann[b], and Molly Reif[c]

a) Director, Joint Airborne Lidar Bathymetry Technical Center of Expertise (JALBTCX)
USACE Engineer, Research and Development Center, Coastal and Hydraulics Laboratory
b) Joint Airborne Lidar Bathymetry Technical Center of Expertise (JALBTCX)
USACE Engineer, Research and Development Center, Coastal and Hydraulics Laboratory
c) Joint Airborne Lidar Bathymetry Technical Center of Expertise (JALBTCX)
USACE Engineer, Research and Development Center, Environmental Laboratory

The number of applications for ALB data has grown exponentially since the first systems became operational in the late 1980's and early 1990's. In those early days, the primary application was nautical charting. Since then, as more systems were developed and fielded, and users gained access to the unique datasets provided by these systems, uses have expanded into a wide variety of coastal engineering and coastal zone management applications. Many of these applications take advantage of the regional-scale, reoccurring elevation and depth data provided by ALB systems. Others utilize semi-automated and automated techniques to extract features from the lidar elevation data, or from lidar waveforms.

Many of the applications that you see in this chapter require data from ancillary systems. One of the primary ancillary data types required for many coastal applications is concurrent topography. It is rare to see a survey requirement that does not include "seamless topography and bathymetry." Some ALB systems collect topographic elevation data concurrently with the bathymetric lidar, either using the green laser or collinear infrared for topography, or by integrating an infrared laser and receive optics into the ALB system. Other systems do not have a built-in topographic capability but are frequently flown with stand-alone topographic lidar sensors. Most ALB sensors are flown with down-looking imagery capability. When ALB systems were first fielded, these cameras were important in the QA/QC phase of data processing for situational awareness. They were video cameras or later, low resolution digital cameras. As the value of imagery grew beyond just assistance in data processing, the quality of cameras integrated with ALB sensors improved. Concurrent high-resolution mosaics are now a common deliverable for airborne coastal surveys.

JALBTCX and others have integrated hyperspectral imagers into their sensor suites, primarily to enable generation of new environmental products. Sensor fusion combines lidar and lidar-derived products with imagery data. One type of sensor fusion that you will see in this chapter is elevation (or depth)-informed thematic mapping. A more complex form of sensor fusion combines lidar depths, reflectivity, and water column attenuation with hyperspectral imagery for production of hyperspectral sea-floor reflectance and water column properties.

This chapter will briefly highlight a number of applications for ALB data that have evolved over the past 25 year of ALB operations: nautical charting, navigation project monitoring, regional sediment management, post-storm response, geomorphological feature extraction, and environmental mapping. It

eCommons (2019) https://doi.org/10.7298/tbxj-3067

is not exhaustive, but gives an overview of the breadth of operational applications for ALB. The chapter closes with a look into future applications.

7.1 Nautical charting

Nautical charting was one of the early drivers for the development of ALB and remains one of the major uses of the technology today. Canada and Australia have a long-standing history of using ALB for nautical charting (since 1985 and 1993, respectively) that continues today. In the US, NAVOCEANO, NOAA, and the National Geospatial-Intelligence Agency (NGA) all use ALB for the production of nautical charts. NAVOCEANO has collected data all over the world since 1996 to support its tactical nautical charting mission in the Bahamas (West and Lillycrop 1999), Mexico (Pope et al. 1997), Honduras, Nicaragua, Belize, Haiti, Martinique, Philippines, Japan, Marshall Islands, Micronesia, Palau, Northern Marianas, Guam, Samoa, New Zealand (Graham et al. 1999), Bahrain, Oman, Portugal (Lillycrop, Pope, and West 2000), Israel, Morocco, and Kenya. NOAA has used ALB for the production of nautical charts for the continental U.S. and in Alaska, Puerto Rico, and the U.S. Virgin Islands. USACE, NAVOCEANO, NOAA and USGS jointly funded a multi-purpose survey mission for the six major Hawaiian Islands in 1999 and 2000 (West 2001) for the creation of nautical charts, coral reef mapping, and flood hazard mapping. The most recent and extensive NOAA ALB surveys are the result of large efforts to update nautical charts in the aftermath of powerful storms like Hurricanes Sandy, Harvey, Irma, and Maria. NOAA frequently uses ALB datasets of opportunity, such as those from the USACE national Coastal Mapping Program in the production of nautical charts.

ALB is used in the production of nautical charts in a number of ways. It may be the sole source of depth data for a chart, or may be used in combination with acoustic, boat-based sensors. In many cases, ALB is operated in advance of boat surveys to help define areas of safe navigation for the survey boats, as well as to provide data for the charts. Some ALB sensors have topographic capability or are paired with a topographic lidar to provide seamless coverage across the land/water interface. The seamless coverage allows for the extraction of shorelines for inclusion on nautical charts. Ancillary camera data enables thematic attribution of shoreline segments. In certain optimal survey conditions, ALB is used to detect objects that are included on nautical charts. Recently, the French Hydrographic and Oceanographic Office (SHOM) started a national program of coastal mapping that supports nautical charting and a number of other uses (Pastol 2011), and South Korean Hydrographic Office (KHOA) has made investments in both ALB surveys and systems. A number of countries issue tenders for contract surveys that include ALB.

7.2 Navigation project monitoring

USACE developed the SHOALS system to augment the existing USACE hydrographic survey capability by providing fast, accurate hydrographic surveys along 40,000 km of federally maintained navigation channels (Lillycrop and Banic 1992). Shoaling, or deposition of sediment in navigation channels, reduces navigability and requires dredging. ALB data is valuable for comparing multiple navigation channel surveys to identify hotspots or morphological trends (Irish and White 1998; Wozencraft and Irish 2000; McClung 1998) that can be leveraged to better maintain these areas through various techniques (channel re-alignment, advanced maintenance dredging, etc.). Figure 7.2.1 shows a topographic and bathymetric DEM of the area near Baker’s Haulover Inlet in southeast Florida. The heavy, black, dashed lines represent the federally authorized channel for this inlet. Lidar datasets collected for this navigation

eCommons (2019) https://doi.org/10.7298/tbxj-3067

channel in June and November 2004, January 2006, and October 2009 were analyzed to estimate a yearly shoaling rate. The high point density of coastal lidar data allow for highly accurate sediment volume calculations. This becomes particularly useful when dealing with tidal inlets and their associated features. The shoaling rate is visualized in the Figure 7.2.1 call-out box (3-D projection), where red indicates areas of higher shoaling and blue indicates areas of little change or even scour. The table shows the average, maximum, and minimum volume of sand in the navigation channel for the four surveys. An alternative analysis is to present channel navigability as a percentage of the congressionally authorized channel depth (L. M. Dunkin and McCormick 2011).

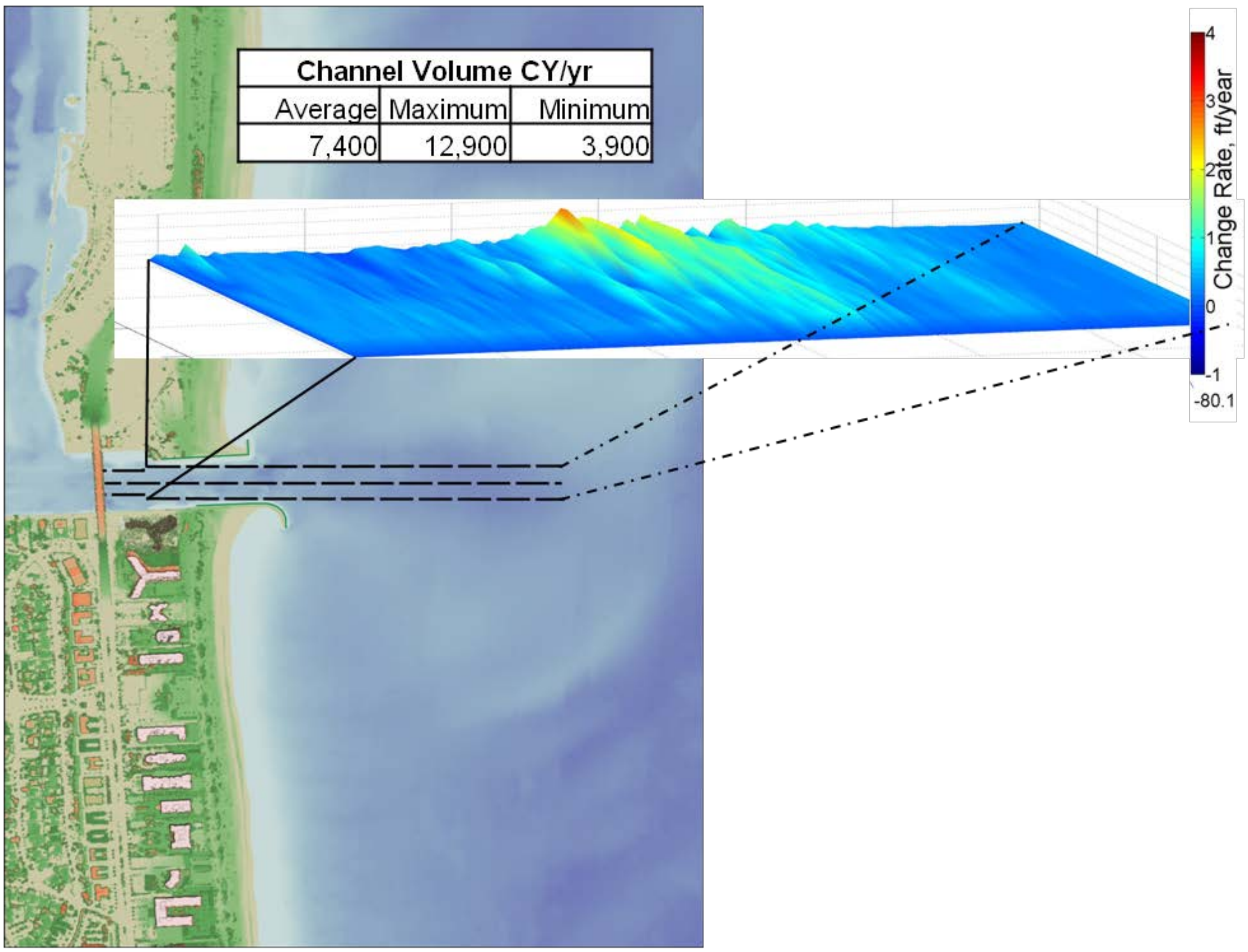

Figure 7.2.1. Channel shoaling rate at Baker's Haulover Inlet, FL. The background image is a topographic and bathymetric DEM of the area. The heavy, black, dashed lines represent the federally authorized channel for this inlet. Lidar datasets collected for this navigation channel in June and November 2004, January 2006, and October 2009 were analyzed to estimate a yearly shoaling rate. The shoaling rate is visualized in the call-out box. Red indicates areas of higher shoaling and blue indicates areas of scour. The table shows the average, maximum, and minimum volume of sand within the authorized channel footprint for the 4 surveys.

Airborne coastal lidar has been used to survey a variety of coastal structures, including navigation structures, like jetties and breakwaters, as well as shoreline protection structures, like detached breakwaters and groins (Irish and White 1998). These structures serve crucial purposes for navigation functionality and coastal protection, but monitoring them can be resource-intensive, requiring manual

eCommons (2019) https://doi.org/10.7298/tbxj-3067

inspection that often only provides a qualitative assessment. Airborne coastal lidar surveys can provide a fast, high-resolution snapshot of a coastal structure. DEMs produced from the lidar data can provide a snapshot of the above and below water condition of a coastal structure and surrounding coastal features. Structure elevation, length, volume, and other measurements can be extracted from DEMs (Reif et al. 2012; Irish and White 1998) to assist with coastal planning and assessments.

Structure functionality often depends on the condition of the structure. A time series of lidar DEMs is useful for structure condition assessments, providing quantification of change over a period of time. Structure volume change, rubble-mound structure side slope steepening, and erosion/deposition adjacent to the structure can be quantified (Irish and White 1998). Metrics extracted from lidar data can be used to monitor structure condition through time. Figure 7.2.2 is a set of cross-sections extracted from 3 years of data for a navigation structure at Hampton Harbor, New Hampshire. In addition, design profiles for navigation channels and structures can be compared to lidar surfaces, and the results may be used in metrics describing how well the channel or structure has maintained its design profile. The charts in Figure 7.2.3 quantify the volume difference between the design profile and cross sections extracted from lidar data collected in 2010, 2011, and 2014. A positive volume is called "cut," where the lidar surface has a higher elevation than the water line. A negative volume is called "fill," where the lidar surface has a lower elevation than the water line. Structure material can be tracked as it is eroded from its original intended use location, and the impacts of coastal structures on coastal processes can be quantified by evaluating changes elevation changes in consecutive lidar datasets (Irish and White 1998; Mohr, Pope, and McClung 1999).

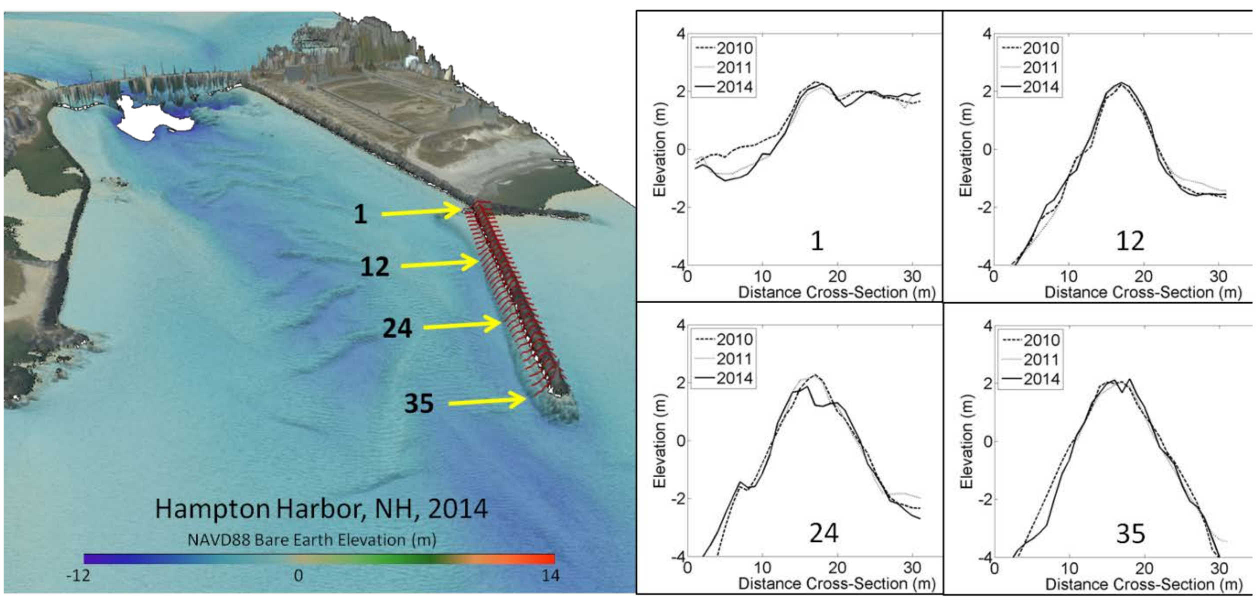

Figure 7.2.2. Cross-sections extracted from 3 years of data at a navigation structure in Hampton Harbor, NH. The cross-sections are numbered 1-35 from landward to seaward, and show how much the structure has changed from 2010-2014.

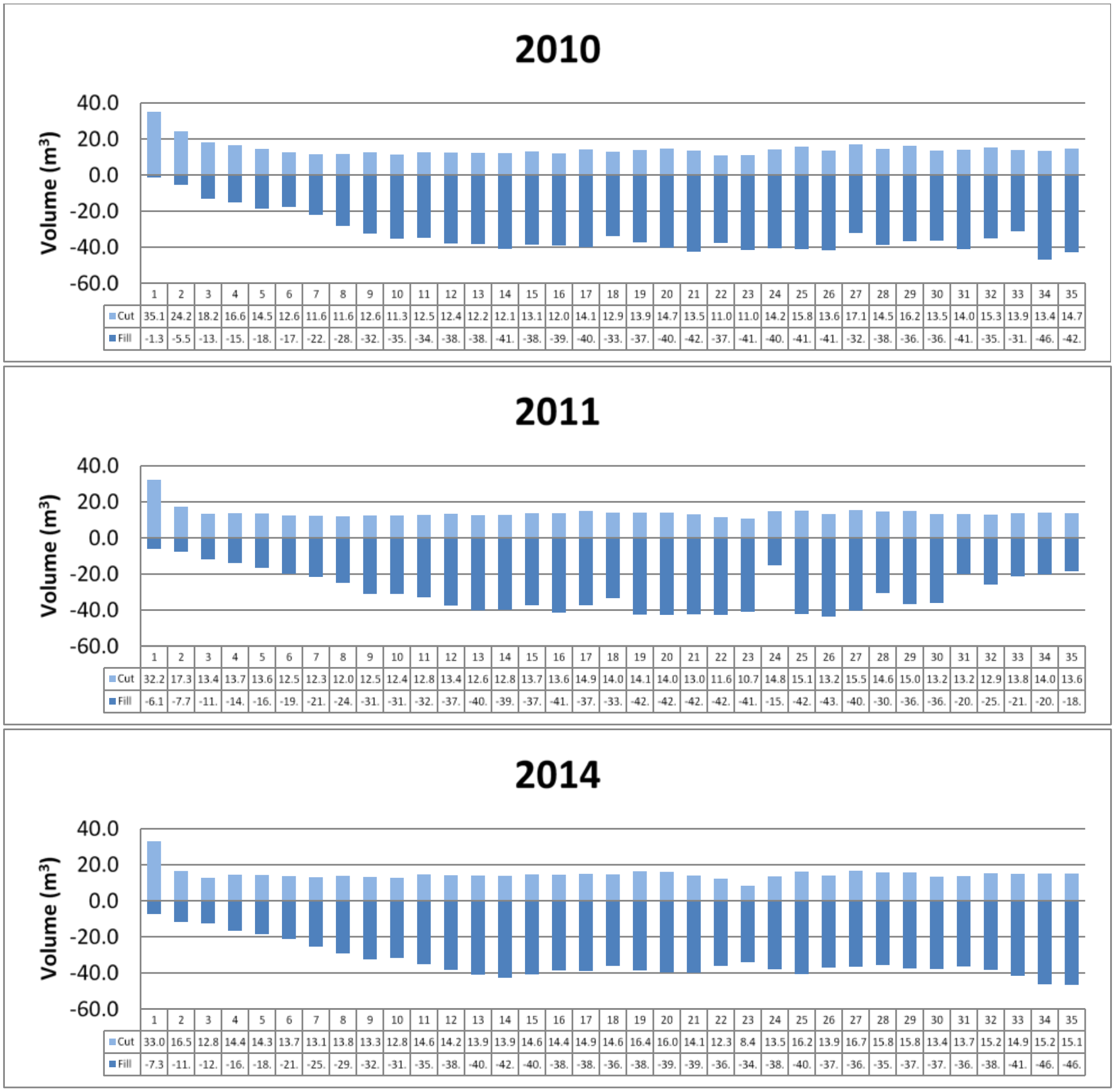

2010

	1	2	3	4	5	6	7	8	9	10	11	12	13	14	15	16	17	18	19	20	21	22	23	24	25	26	27	28	29	30	31	32	33	34	35
Cut	35.1	24.2	18.2	16.6	14.5	12.6	11.6	11.6	12.6	11.3	12.5	12.4	12.2	12.1	13.1	12.0	14.1	12.9	13.9	14.7	13.5	11.0	11.0	14.2	15.8	13.6	17.1	14.5	16.2	13.5	14.0	15.3	13.9	13.4	14.7
Fill	-1.3	-5.5	-13.	-15.	-18.	-17.	-22.	-28.	-32.	-35.	-34.	-38.	-38.	-41.	-38.	-39.	-40.	-33.	-37.	-40.	-42.	-37.	-41.	-40.	-41.	-41.	-32.	-38.	-36.	-36.	-41.	-35.	-31.	-46.	-42.

2011

	1	2	3	4	5	6	7	8	9	10	11	12	13	14	15	16	17	18	19	20	21	22	23	24	25	26	27	28	29	30	31	32	33	34	35
Cut	32.2	17.3	13.4	13.7	13.6	12.5	12.3	12.0	12.5	12.4	12.8	13.4	12.6	12.8	13.7	13.6	14.9	14.0	14.1	14.0	13.0	11.6	10.7	14.8	15.1	13.2	15.5	14.6	15.0	13.2	13.2	12.9	13.8	14.0	13.6
Fill	-6.1	-7.7	-11.	-14.	-16.	-19.	-21.	-24.	-31.	-31.	-32.	-37.	-40.	-39.	-37.	-41.	-37.	-33.	-42.	-42.	-42.	-42.	-41.	-15.	-42.	-43.	-40.	-30.	-36.	-36.	-20.	-25.	-21.	-20.	-18.

2014

	1	2	3	4	5	6	7	8	9	10	11	12	13	14	15	16	17	18	19	20	21	22	23	24	25	26	27	28	29	30	31	32	33	34	35
Cut	33.0	16.5	12.8	14.4	14.3	13.7	13.1	13.8	13.3	12.8	14.6	14.2	13.9	13.9	14.6	14.4	14.9	14.6	16.4	16.0	14.1	12.3	8.4	13.5	16.2	13.9	16.7	15.8	15.8	13.4	13.7	15.2	14.9	15.2	15.1
Fill	-7.3	-11.	-12.	-16.	-18.	-21.	-25.	-29.	-32.	-31.	-35.	-38.	-40.	-42.	-40.	-38.	-38.	-36.	-38.	-39.	-39.	-36.	-34.	-38.	-40.	-37.	-36.	-35.	-37.	-37.	-36.	-38.	-41.	-46.	-46.

Figure 7.2.3. Structure volume above and below the water line computed from lidar data collected in 2010, 2011, and 2014. Each bar in the graph represents one of the cross-sections shown in Figure 7.2.2, numbered 1 to 35 landward to seaward, and left to right in the graph. A positive volume is called "cut," where the lidar surface has a higher elevation than the water line. A negative volume is called "fill," where the lidar surface has a lower elevation than the water line.

Quantifying nearshore coastal change around navigation channels and structures can improve navigation project management by providing an understanding of erosion and deposition patterns in the immediate vicinity. Ebb shoals are important morphological features that need to be quantified to determine the amount of sediment that may be available for nourishment of downdrift beaches through natural sediment bypassing and/or used as a borrow source for projects. In addition, the ebb shoal volume, compared to a theoretical no-inlet system, is important to quantify the inlet sink effect for sediment budgets.

eCommons (2019) https://doi.org/10.7298/tbxj-3067

Automated procedures for identifying watersheds in a hydrological context are used to identify the boundary of the shoal features. The ebb shoal boundary for Big Sarasota Pass, Florida, is shown by the black hashed polygonal areas in Figure 7.2.4. This footprint is used for volume and volume change calculations based on ALB surveys from June and November of 2004, January 2006, and June 2010, shown in the table. At this inlet, sediment transport is from north to south as evidenced by offset ebb shoal and drumstick barrier island to the south. Notice the channel (shown in heavy black lines) bisects the ebb shoal in an area that is shallower than the more southerly portion as the tidal flow naturally scours out the portion of the channel and moves in a southerly direction.

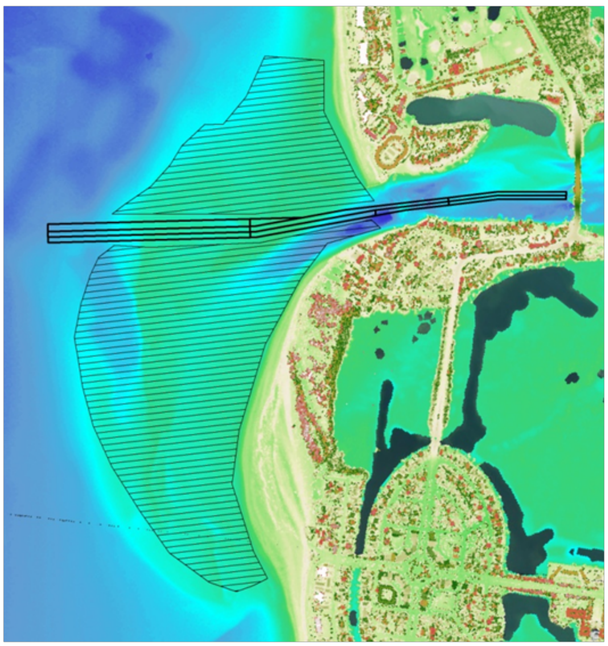

Volume Change (CY)

Survey	Total
6/2010--6/2004	6,932
6/2010--1/2006	-89,785
6/2010--11/2004	-65,302
1/2006--6/2004	147,968
1/2006--11/2004	292,443
11/2004--6/2004	-163,402

Figure 7.2.4. Ebb shoal volume calculations for Big Sarasota Pass, FL. The black hashed polygonal areas are the boundary of the ebb shoal as determined by automated routines that operate on lidar DEMs. The heavy black lines demarcate the authorized alignment of the Federal navigation channel at this inlet. The table is a series of volume changes calculated between lidar datasets within the ebb shoal boundary.

7.3 Regional sediment management

USACE manages navigation, coastal storm damage risk reduction, and environmental restoration projects in the coastal zone. Until the late 1990's these projects were funded and managed as individual units, and in some cases, individual navigation structures were managed separately from the navigation channels they were designed to stabilize. Regional Sediment Management (RSM) is a management construct in which all the projects in a region, where region is defined by coastal processes, are managed as a holistic system (Lillycrop, et al. 2011). The main goals of RSM are to realize operational efficiencies among projects, and to manage in concert with natural processes to minimize the effect of management actions like dredging and the placement of dredged materials. In many cases, environmental benefits are realized through RSM.

eCommons (2019) https://doi.org/10.7298/tbxj-3067

Managing projects on a regional basis requires regional datasets. Sediment movement, deposition, and erosion along a coastline is a regional process by nature, therefore, efforts to manage and understand sediment dynamics in the coastal zone must be conducted on such a scale. The regional nature of airborne coastal lidar makes it an ideal tool for conducting surveys for RSM on a large scale (Wozencraft and Irish 2000). The USACE National Coastal Mapping Program (NCMP) was initiated in 2004 to produce the recurring, regional, high-resolution, high-accuracy, data necessary to implement regional sediment management practices at USACE coastal projects (Wozencraft and Millar 2005).

Sediment budgets are a fundamental part of the RSM strategy, allowing for quantification of sediment movement and potential impacts of projects across a coastal region. Sediment volume change calculated within delineated sediment budget ‘cells’ are combined with knowledge of transport directions and dredging or placement activity to develop a detailed picture of sediment sources, sinks, and fluxes for the area of interest (Rosati 2005). Volume changes can be derived for sections of a study area to quantify sediment inputs and outputs on a fine scale (Irish and Lillycrop 1997; Irish, Lillycrop, and Parson 1997; Wozencraft 2001; Wozencraft and Irish 2000). These volumes can then be incorporated into regional or project-scale sediment budgets (West and Wiggins 2000). Multiple coastal lidar datasets collected in an area of interest can quantify coastline response to known variations in sediment supply, such as a sediment deficit (Xhardé, Long, and Forbes 2011) to further inform sediment budget development. Comparison of bare-earth topo-bathy DEMs quantifies elevation and sediment volume changes on the beach and nearshore and can help identify sand transport pathways through the coastal zone (Irish and Lillycrop 1997; Mohr, Pope, and McClung 1999; Wozencraft 2001; Wozencraft and Lillycrop 2006). Sediment transport within the coastal zone can also be calculated using bathymetry derived from airborne coastal lidar surveys. Along with wave data, both the cross-shore and along-shore transport rates can be inferred from lidar bathymetry data (Irish and White 1998).

Initial studies applying airborne coastal lidar to assess sediment movement on a regional scale were conducted by the RSM Demonstration Program in the USACE Mobile District. As a part of this program, repeat, regional lidar topobathy datasets collected along 360 km of Gulf of Mexico shoreline, from Dauphin Island, Alabama, in the west to Apalachicola Bay, Florida, in the east were included in a single RSM region (Wozencraft and Irish 2000). Four airborne lidar datasets (Oct. and Nov. 1995, Dec. 1996, Nov, 1997) collected by the SHOALS-200 were utilized to conduct a detailed, quantitative sediment management assessment of East Pass inlet, Florida. Qualitatively, the location of the ebb shoal, sediment dredging, placement, as well as the development of scour holes associated with navigation structures and channel currents were observed. Elevation difference plots were created between datasets each dataset to quantify elevation changes over time across the inlet. A volumetric analysis conducted within each of six areas including the channel, adjacent beaches, and ebb shoal produced the volume of sediment lost or added to each area within each time slice (Figure 7.3.1, Table 7.1). Trends observed from this data coupled with qualitative observations from the digital elevation models and elevation difference plots provide a full picture of sediment movement through the system. This analysis illustrates the how airborne coastal lidar datasets can provide useful qualitative and quantitative sediment volume and morphological data.

eCommons (2019) https://doi.org/10.7298/tbxj-3067

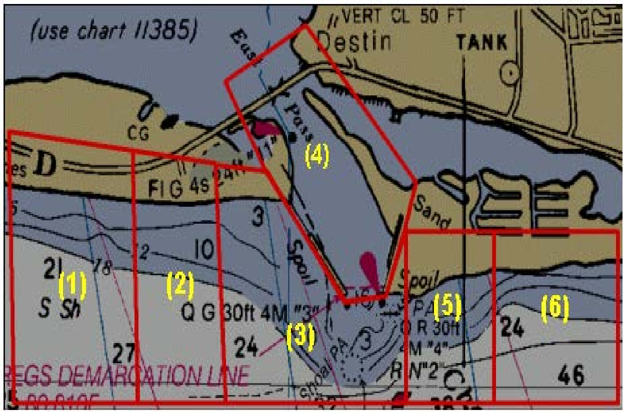

Figure 7.3.1. East Pass, Florida. Red lines delineate sediment budget cells for sand volume calculations (Wozencraft and Irish 2000).

Table 7.1. *Sand volume computations for East Pass, Florida. Volumes are thousands of m3.* (Wozencraft and Irish 2000)

	1	2	3	4	5	6
1995	X	X	1.6	5.3	X	X
1995-1996	X	X	-8.3	-10.8	X	X
1996-1997	-13.4	-5.2	-11.8	-1.2	-1.7	-8.0

To support engineers using lidar-derived volume changes in their sediment budgets, NCMP began developing a standard method for analyziang beach change in 2010. The method utilizes NCMP datasetsand produces volume and shoreline change in shore-perpendicular bins, for entire regions of coastline. The methodology was refined through several years of operations and in 2016 was incorporated into an ARCGIS extension called the JALBTCX Toolbox. This methodology can be used across many coastal regions, and produce consistent data products for coastal assessments and sediment volume change analysis (Robertson et al. 2018). The JALBTCX Toolbox was used to compute volume and shoreline change between the NCMP data collected in 2004/5 with NCMP data collected in 2009/2010 for the eastern Gulf of Mexico and Atlantic coast shorelines.

7.4 Post-storm response

The volume and shoreline change tools in the JALBTCX Toolbox have been used most extensively in recent years to quantify changes due to coastal storms, specifically Hurricanes Matthew (2016), Irma (2017) Maria (2017), Florence (2018), and Michael (2018). Airborne coastal lidar surveys have been flown after major storm events since the mid-1990's. These early surveys evaluated storm impacts at the project scale for the Federal navigation project at East Pass, FL (Irish et al. 1996), beach nourishment project at Longboat Key, FL (Irish and Lillycrop 1999), and a 40 km stretch of FL Atlantic coast (Zhang et al. 2005). Response to the 2004 and 2005 hurricane season, which saw the landfall of Hurricanes Charley, Frances, Ivan, Jeanne, Dennis, Katrina, and Wilma, marked a change to larger scale impact assessments using airborne coastal lidar. The USGS flew the NASA EAARL system before and after some of these storms to quantify the impacts of the storms for their Hurricane and Extreme Storm Impact Studies (Sallenger, Wright, and Lillycrop 2005; Sallenger et al. 2006). USACE used the EAARL data and collected data with CHARTS for many of these storms as well. The data were used in developing Project Impact Reports that USACE uses to request funds from Congress for rebuilding projects to their pre-storm or design condition (Wozencraft and Millar 2005) and to quantify land cover changes (Reif, Macon, and Wozencraft 2011).

eCommons (2019) https://doi.org/10.7298/tbxj-3067

The airborne coastal lidar mapping response to Hurricane Sandy was the first lidar response that was more tactical in nature. USGS and USACE put together a large, multi-state, post-storm response effort where the goal was to not only collect the data as quickly as possible after the storm, but to also deliver the data in a matter of days after collection for use by emergency responders. EAARL and CZMIL deployed in New Jersey and New York to support this effort (Wozencraft 2013). The post-storm data were compared with data collected before the storm along the entire stretch of coastline. The coastline was divided into analysis sections and a paper map product was developed for each (Figure 7.4.1). The volume and shoreline change analysis were performed using an early version of the JALBTCX Toolbox, and the paper maps were generated using a combination of ARCGIS and Excel.

CZMIL and the JALBTCX Toolbox were more recently deployed after Hurricanes Matthew, Irma, Maria, and Michael. After Hurricane Matthew, JALBTCX deployed two CZMIL systems to collect data for the coastlines of Florida, Georgia, South Carolina, North Carolina, and Virginia, in the period of one month. These data supported USACE in development of Project Impact Reports for Federal beach projects in the area, and to assess the broader impact of the storm. Data for federal beach projects were delivered within days of collection, and data for the entire survey area were delivered within a month of the end of survey. The JALBTCX Toolbox produced shoreline and volume change for the entire region that were published in an interactive web tool (https://www.arcgis.com/home/item.html?id=d1ee0da4887046edbc9ff05c66d40708). FEMA requested JALBTCX surveys for the east coast of Florida, the Florida Keys, and Collier County of the west coast of Florida in the aftermath of Hurricane Irma. The intent of these surveys was to determine eligibility of coastal communities for public assistance grants to install emergency protective measures. Eligibility is based on elevation above the 5% flood exceedance level, and the amount of assistance was based on the quantity of sand needed to restore the beach to this elevation, both of which were determined from the lidar data. For the post-Irma surveys JALBTCX delivered final data products within five days of collection for the entire area, and volume change analysis was complete a month from the end of survey. FEMA funded JALBTCX surveys and computation of beach sand volume loss along the coastline of Puerto Rico in the aftermath of Hurricane Maria. The data and computed volumes support the Natural and Cultural Resources Sector in their beach erosion assessment for the Puerto Rico Recovery Plan. After Hurricane Michael, FEMA and the State of Florida jointly funded JALBTCX surveys along the impacted area of the Florida Panhandle. The data and change analysis supported local communities in assessing damage from the storm, and in preparing for future storm events.

7.5 Geomorphological feature extraction

Various techniques have been developed through the years for the extraction of features from coastal lidar datasets, for a variety of applications. Some of the features that will be discussed in this section are shown in the graphic in *Figure 7.5.1*: shoreline, dune crest, dune toe, and dune volume. Others are beach width, which is the distance between the dune toe and the shoreline; bluff or cliff edges, which are an analog of the dune crest, but on uplifted rocky and cohesive sediment coastlines; and shoreline change, which is a comparison of position of the shoreline between two surveys.

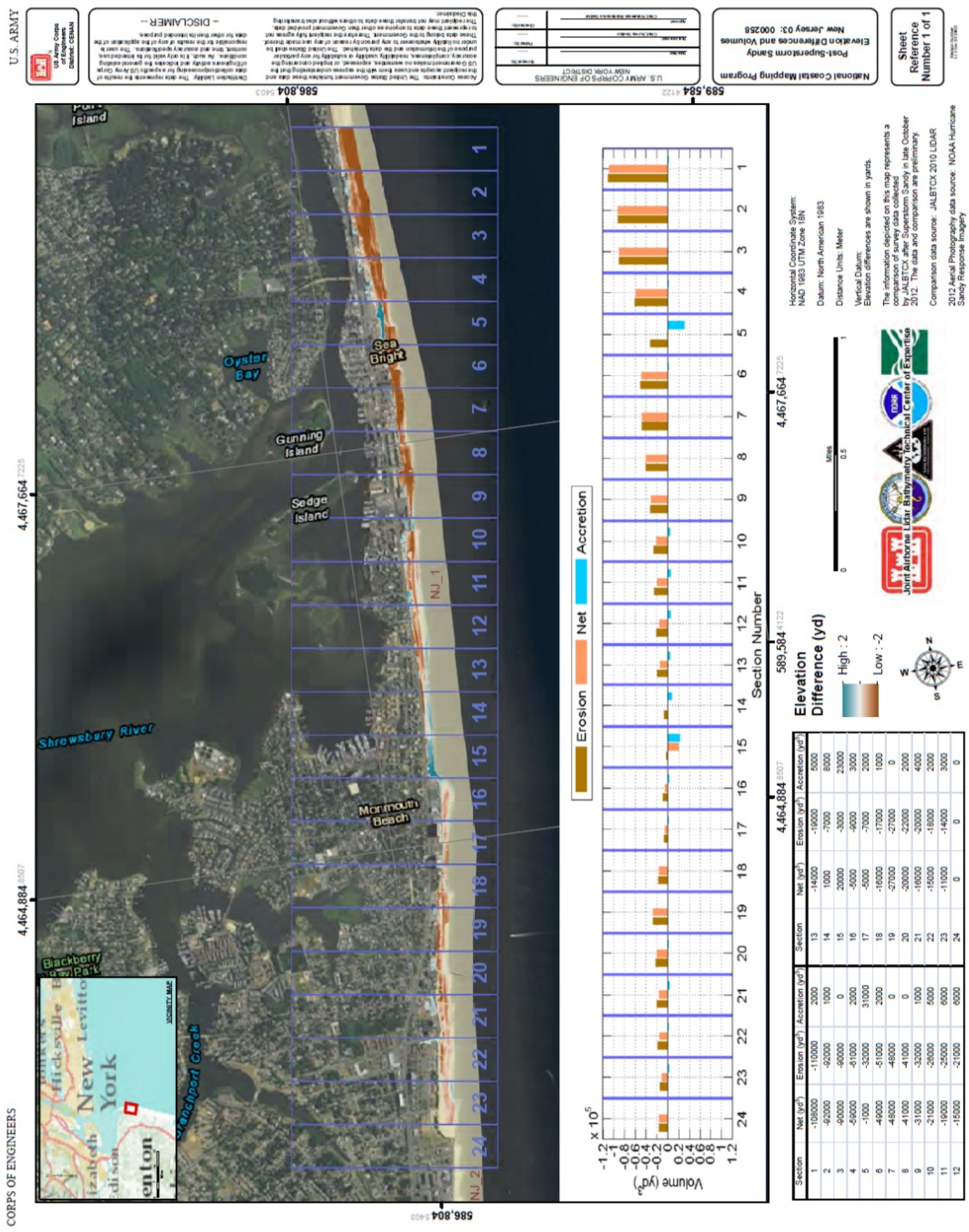

Figure 7.4.1. JALBTCX preliminary change detection product near Sea Bright, New Jersey. The brown and blue overlay near the shoreline indicates where erosion (brown) and accretion (blue) have occurred. The graph and table give quantities of sand volume change (Wozencraft 2013).

eCommons (2019) https://doi.org/10.7298/tbxj-3067

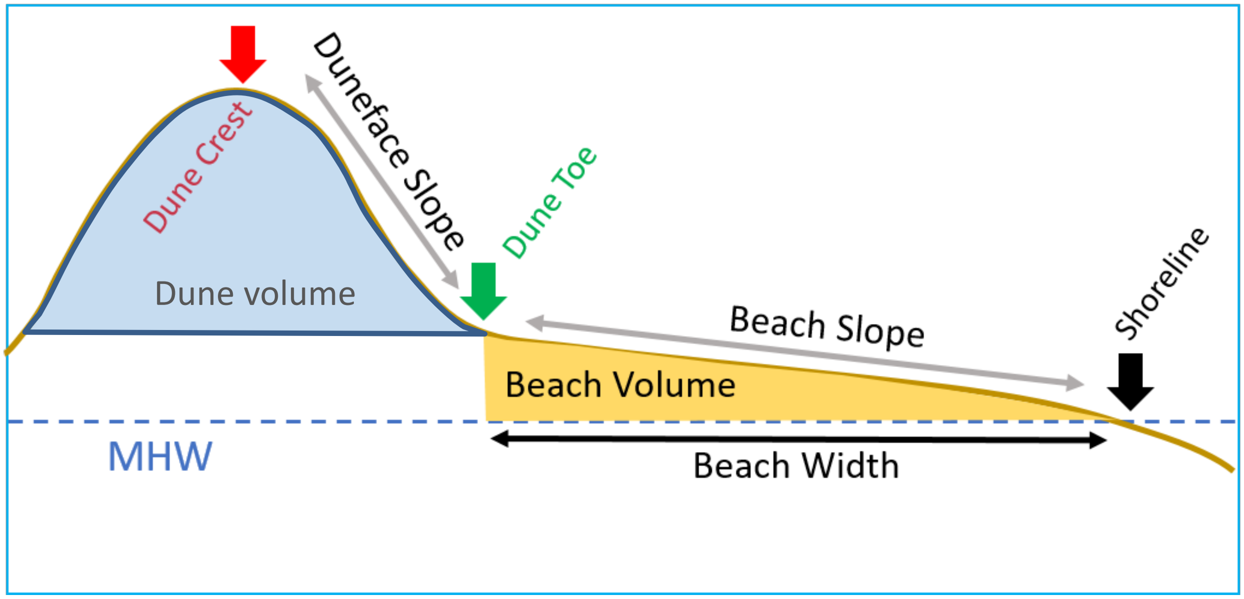

Figure 7.5.2. Schematic of a cross-shore profile. Inflection points help identify the location of the dune crest and dune toe. The shoreline location is the zero elevation on the profile relative to a specified vertical datum. Dune volume is bounded by the dune toe and seaward-most line of infrastructure.

7.5.1 Shorelines and shoreline change

The term shoreline nominally refers to the geographic location of the land-water interface. Because this location changes with the tides, winds, and waves, it is common practice to develop a shoreline that is aligned with a particular tidal or orthometric datum, depending on end use of the derived shoreline vector. Uses of shoreline and shoreline change data include:

- Definition of legal boundaries, as in the National Shoreline produced by NOAA's National Geodetic Survey, and included on nautical charts (Aslaksen et al. 2012)
- ascertain the temporal and spatial variability alongshore erosion hotspots (List, Farris, and Sullivan 2006) and their causes (McNinch 2004; Schupp, McNinch, and List 2006)
- monitoring shorelines in the vicinity of Federal navigation projects (Irish and White 1998; Stauble 2003)
- monitoring performance of coastal storm damage reduction projects (Bocamazo, Grosskopf, and Buonuiato 2011).
- identifying long-term coastal change hazards (Stockdon et al. 2002).

There are two main approaches for extracting shoreline from lidar data, on is DEM-based and the other is profile-based. The DEM approach uses spatial analysis tools in a GIS to extract a contour at the desired elevation. If the DEM is vertically referenced to the desired datum, the zero contour is extracted (White 2007; White et al. 2011) Otherwise, an elevation contour coincident with the difference between the vertical reference of the DEM and the desired datum elevation is selected, such as mean high water

eCommons (2019) https://doi.org/10.7298/tbxj-3067

(Robertson, William et al. 2004). Profile-based approaches (Stockdon et al. 2002; Weber, List, and Morgan 2005) locate the intersection of a local MHW datum elevation along a series of lidar-derived beach profiles. The shoreline is generated by connecting these locations in the alongshore direction.

7.5.2 Dune and depositional coastal features

Topography derived from airborne lidar surveys along the coast can be used to assess dune features, including their volumes and locations (Gares, Wang, and White 2006; Wozencraft et al. 2018). Storm surge channels, formed by erosion during storms, as well as relict beach ridges, indicating past shoreline progradation, can be observed using lidar topography, as was done along Galveston Island, Texas to assess coastal erosion (Wallace, Anderson, and Rodriguez 2009). Beach slope and its alongshore variability was derived from lidar data for a section of coastline in Paspébiac, Quebec, providing information about wave action on the shoreline (Xhardé, Long, and Forbes 2011). Tracking the growth and development of spits and other depositional features is possible with this data as well (Xhardé, Long, and Forbes 2011). Four topobathy lidar datasets capturing the Ship Island barrier island, located along the Mississippi Gulf Coast, USA, were used to track changes in dune, beach, and subaqueous features over several years (Eisemann et al. 2018). Automated processes have been developed to extract the location of the dune peak, the mean and max dune peak heights, and the beach width for a certain stretch of coast (L. M. Dunkin and McCormick 2011).

The USGS has been extracting dune parameters from coastal lidar data for a number of years to examine the vulnerability of beaches to inundation during hurricanes (Stockdon, Doran, and Sallenger 2009). The general approach is to calculate inflection points on cross-shore profiles extracted from lidar data at certain intervals along the coast. Dunes act as the first natural line of defense against waves and runup during storm events. Locating the dune fields and monitoring change or recovery after a storm is important for understanding the level of protection that is available and can be used to plan for improvements that may be needed to increase upland protection. USGS delivers operational forecasts of the probability of wave collision, overwash, coastal inundation, and total water levels, based on dune metrics extracted from lidar datasets.

The location of the dune crest, dune toe, and shoreline may be presented in a variety of ways, such as dots or lines on a map (Figure 7.5.2). While shoreline has a constant zero elevation, the elevation of the dune crest and dune toe vary alongshore, and can be presented in a graph along with other parameters, such as beach width (Figure 7.5.3). Beach width can be calculated as the distance from the shoreline to the dune toe (Figure 7.5.1). Plotting extracted dune crest heights within a geographical context can demonstrate the alongshore variability in dune crest height, and how individual dune crest heights relate to the mean for a region. With repeat DEM datasets, dune elevation and location changes can be mapped to better understand the dynamics of the dune system in a region.

eCommons (2019) https://doi.org/10.7298/tbxj-3067

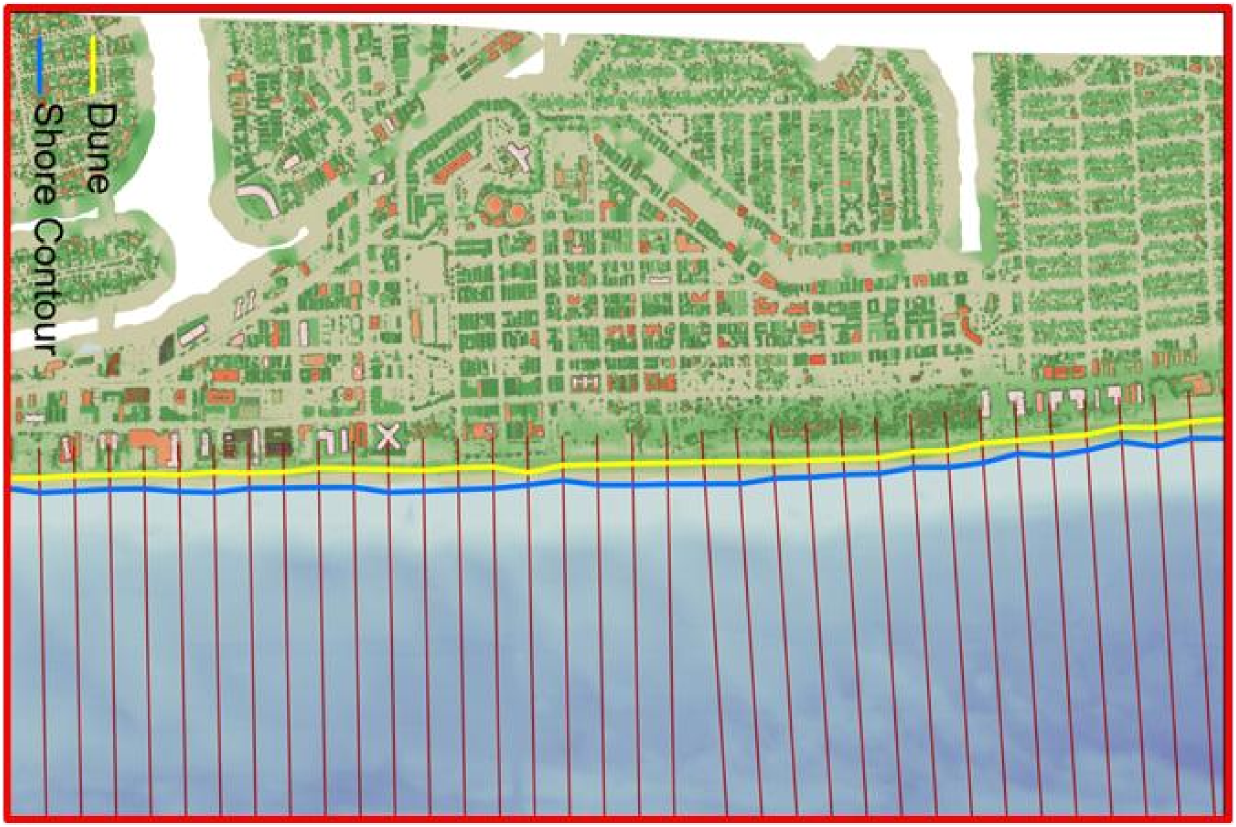

Figure 7.5.3. Dune crest (yellow) and shoreline location (blue) for a small section (3 km) of the Florida Panhandle east of East Pass (Destin). The red vertical lines indicate the location of cross-shore profiles from which the dune crest and shoreline locations were extracted.

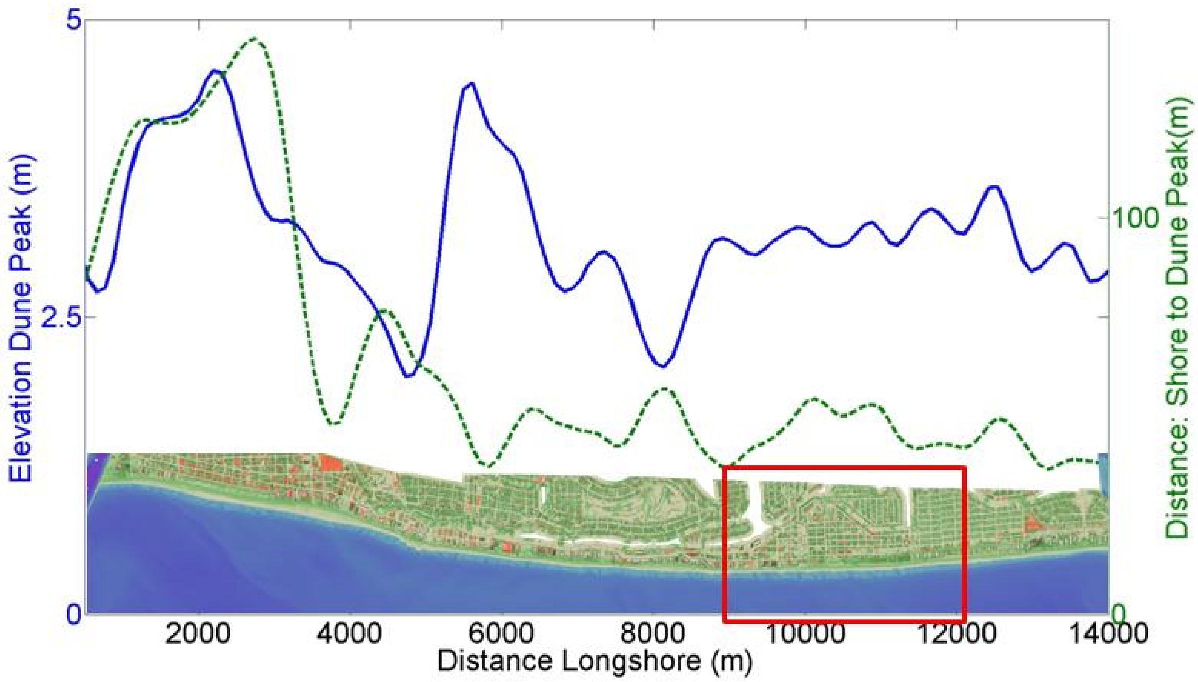

Figure 7.5.4. Alongshore variability in dune crest height (blue) and beach width (green) for a larger section (14 km) of the Florida Panhandle east of East Pass (Destin). The red box is the area shown in Figure 7.5.2.

eCommons (2019) https://doi.org/10.7298/tbxj-3067

7.5.3 Bluff and cliff edge detection

Bluff erosion is the primary source of sediment in the nearshore zone along coastlines in the Great Lakes region of the United States and Canada, (Baird 2002). Cliff erosion also provides an important source of sediment to the littoral zone, typically coupled with riverine and gully inputs (Young and Ashford 2006). Bluff and cliff edge retreat rates can be converted to volume contributions to the local sediment budgets using simple assumptions (Baird 2002; Young and Ashford 2006). Bluff and cliff edges both mark the line of landward retreat before land and property is lost due to erosion, so the ability to assess these geomorphic features and compare the results across multiple surveys is invaluable for understanding the condition and vulnerability of these regions (Reif et al. 2013). Airborne coastal lidar data has been used to determine bluff edges using both manual interpretation of DEMs and automated procedures similar to those described above for dune crests. In the manual procedure, the bluff edge is hand digitized from hillshade renderings of coastal lidar DEMs (Hapke and Reid 2007; Hapke, Malone, and Kratzmann 2009). Automated methods can identify the bluff edge as the location where the variation in slope along a lidar elevation transect is at a maximum (Liu et al. 2009).

JALBTCX has improved these automated processes by extracting the bluff edge from bare earth DEMs, which greatly reduces lidar pre-processing, and excludes buildings and vegetation from the analysis to find the bluff edge. Transects are extracted from the bare earth DEMs with spot elevations spaced 1 meter along the profile and 10 meter alongshore spacing between profiles. Transects are analyzed profile-wise with a custom set of algorithms to find the location of the maximum change in slope in addition to meeting specific threshold values that are implemented to prevent deviations in the bluff line from being extracted. The bluff edge location for each transect is joined with the neighboring points to create a continuous line for the region. The automated process is demonstrated for a portion of Lake Erie, NY using bare earth DEMs generated from lidar data collected during the 2007 NCMP survey (Figure 7.5.4). Bluff edge change rates were calculated using the GIS extension, Digital Shoreline Analysis System (DSAS), developed by the USGS (Thieler et al. 2009) to compare the lidar derived bluff line to an 1874 digitized bluff line. The spatial variability of the bluff edge change rates makes having the lidar elevation data, particularly the bare earth DEMs, invaluable for monitoring efforts. Bluff edge change rates can be used to assist coastal planners and engineers for sediment budget analyses, coastal mapping, land use planning, and permitting.

eCommons (2019) https://doi.org/10.7298/tbxj-3067

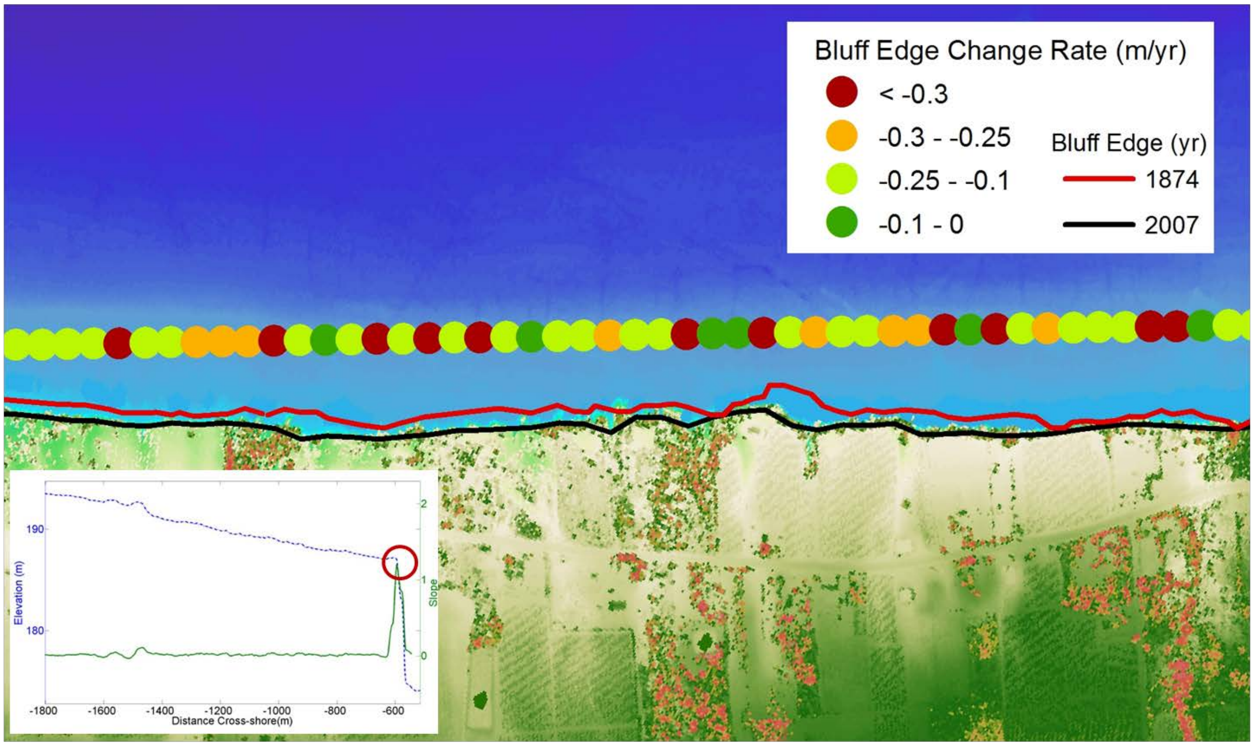

Figure 7.5.5 . Long-term bluff edge change rate for a portion of Lake Erie (New York) and an example profile plot of the elevation (blue dashed line) and slope (green line) where the location of the maximum slope (bluff edge) is identified (red circle). (From Reif et al. 2013).

Similar automated detection methodologies used on seacliffs incorporate further advancements to accommodate the more complex geometries of cliffs, with terraces and varying slope gradients (Palaseanu-Lovejoy et al. 2016).

7.6 Environmental mapping

Environmental mapping with airborne coastal lidar falls into the two broad categories of land cover classification and seafloor classification. Some environmental mapping is performed using ALB elevation and depth data alone. Studies of seafloor complexity calculate rugosity (topographic roughness) from ALB depth data (Walker, Riegl, and Dodge 2008), at varying spatial scales (Zawada and Brock 2009; Pittman, Costa, and Battista 2009). Lidar waveform shape parameters used in concert with ALB depths have informed seafloor classifications of seagrass (C.-K. Wang and Philpot 2007) bottom sediment and algal cover (Cottin, Forbes, and Long 2009), and a number of estuarine supralittoral, intertidal, and subtidal habitats (Chust et al. 2010). Lidar intensity data, a measure the light energy returning from the seafloor, identified areas of shell fragment off the coast of New Jersey (C.-C. Wang and Tang 2012), and sand laden with tailings from copper mining (Reif et al. 2013). ALB-derived measurements of seafloor complexity have demonstrated skill in predicting diversity and abundance of fish and corals (Pittman, Costa, and Battista 2009) and species diversity of benthic communities (Collin, Long, and Archambault 2011). A series of metrics extracted from EAARL lidar waveforms collected over land describe

eCommons (2019) https://doi.org/10.7298/tbxj-3067

vegetation communities (Nayegandhi et al. 2006; Palaseanu-Lovejoy et al. 2009). These projects utilize a variety of supervised, unsupervised, and machine learning techniques.

The integration of hyperspectral imagers with ALB sensors enables elevation-informed thematic mapping for environmental applications over land. Combining the height information in lidar data with spectral information available in imagery improves the capability of both data sets to characterize environmental conditions in the coastal zone. A supervised classification combining lidar elevation with hyperspectral image band ratios identified invasive Phragmites australis on a dredge material placement site (Reif et al. 2013). Future surveys and classifications may be used to determine effectiveness of herbicide treatments. A series of lidar and hyperspectral image surveys were collected over the south shore of Lake Pontchartrain in New Orleans, immediately after Hurricane Katrina and in the following years. These datasets were used to develop a highly-automated decision tree classifier that uses height-above-ground calculated from lidar DEMs and hyperspectral bands and band ratios to produce a basic landcover classification. Analysis of the Lake Pontchartrain landcover classifications documents changes in vegetation communities and housing in this hurricane impacted area (Reif, Macon, and Wozencraft 2011). New techniques have been developed to quantify dune vegetation density, wherein dune features extracted from lidar DEMs constrain image analysis to identify pixels that contain vegetation, then computes dune density with neighborhood statistics (Wozencraft et al. 2018).

Sensor fusion of ALB and hyperspectral imagery enables a number of new products. Spectral optimization algorithms use lidar-derived depth, attenuation, and bottom reflectance as constraints in the spectral decomposition of the water column and seafloor (Kim, Park, and Tuell 2010). Using this method, the atmosphere, water column, and seafloor signals are decomposed into their component constituents, and incorporated into the radiative transfer equation inversion process through a series of analytical and empirical relationships, all well-established in the ocean optics community (Wozencraft and Park 2013). The results of this approach are spectral water-leaving reflectance, water column attenuation, *Chlorophyll a* and colored dissolved organic matter absorption, spectral seafloor reflectance, and abundance images depicting the proportionate contributions of seafloor constituents in each pixel based on input bottom spectra (Aitken et al. 2010). Spectral seafloor reflectance images generated using spectral optimization were analyzed to discriminate between submerged vegetation species of eelgrass and macroalgae in support of nearby dredging operations (Reif et al. 2012). The eelgrass maps produced using this product exhibited more detail and granularity than maps produced through heads-up digitizing of aerial photography. Spectral seafloor reflectance images and ALB depths informed a benthic mapping study in support of RSM off the west coast of Maui Figure 7.6.1. The goal of the study was to locate sand to support RSM initiatives, and sensitive habitats that might be impacted by dredging and placement operations.

eCommons (2019) https://doi.org/10.7298/tbxj-3067

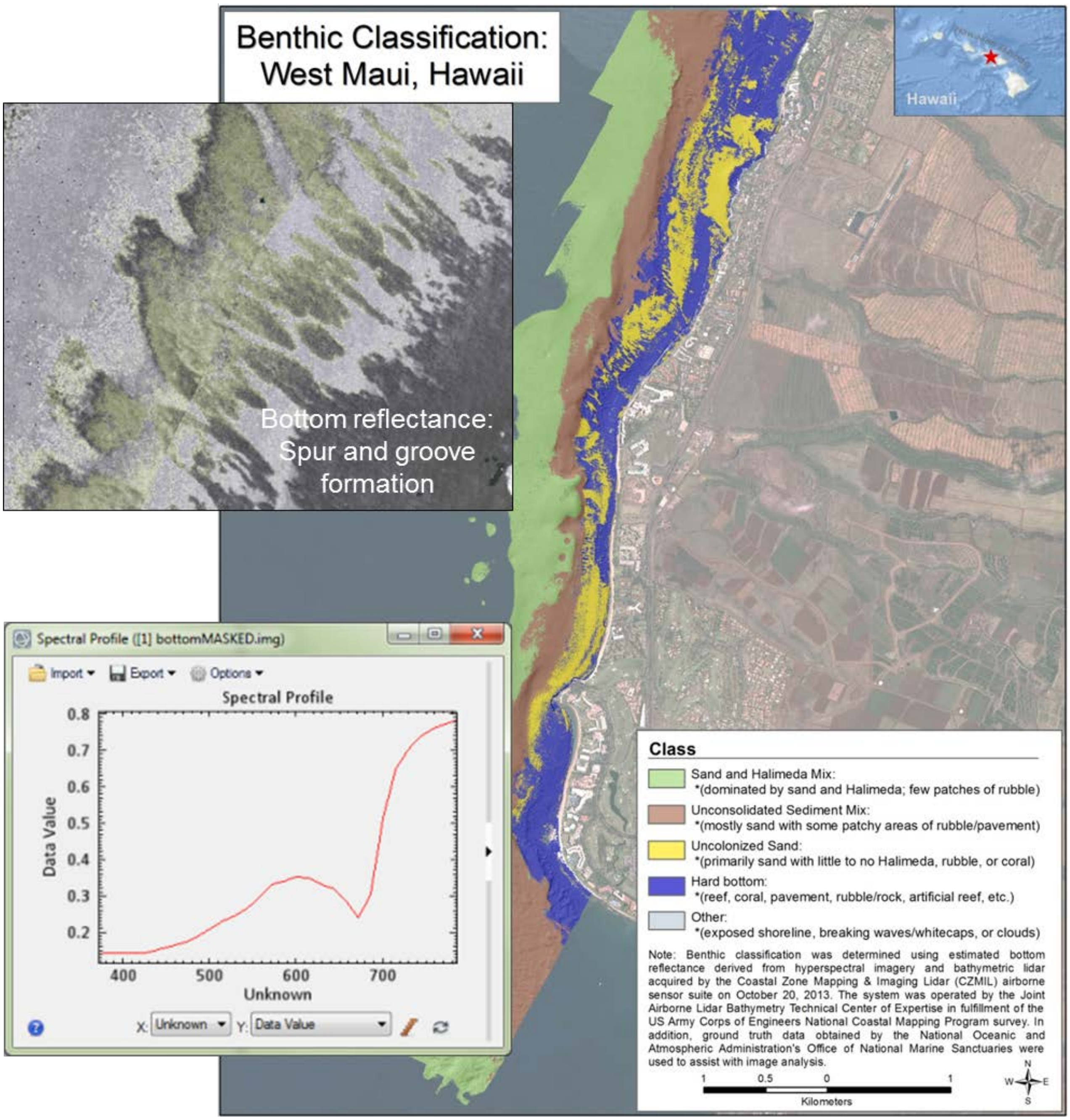

Figure 7.6.1. Benthic classification map generated for regional sediment management study off the coast of west Maui, identifying areas of sand and Halameda mix, unconsolidated sediment mix, uncolonized sand, and hard bottom.

7.7 Summary and future work

This chapter has identified a number of applications for airborne coastal lidar, used alone, or in concert with ancillary passive imagers in a sensor fusion paradigm: nautical charting, navigation project monitoring, regional sediment management, post-storm response, geomorphological feature extraction,

eCommons (2019) https://doi.org/10.7298/tbxj-3067

and environmental mapping. The relative speed with which these technologies can collect very large areas make them ideal tools for change detection and coastal characterization at both local and regional scales. Recent work combines the products and applications presented in this chapter to support applications such as landscape evolution modeling (Reif and Swannack 2014) and habitat suitability models for sea turtle nesting (L. Dunkin et al. 2016; Yamamoto et al. 2012).

Synoptic views of coastal condition can be compiled from a number of the products demonstrated in this chapter. One example is a coastal dashboard that visualizes indices comprising features extracted from airborne coastal lidar and ancillary datasets (Wozencraft et al. 2018). This is useful for coastal practitioners as they plan for projects or monitor a stretch of coast. The example in Figure 7.7.1 shows a geomorphological index that includes beach width, dune height, and shoreline change. The environmental index indicates presence of critical habitats including seagrass, wetlands, and dune vegetation. The human use index looks at coastal development in terms of impervious surfaces. The pie charts show indices for navigation projects including stability of offshore shoals features, how well structures match their design profiles, and how much of the navigation channel is at or below the authorized channel depth.

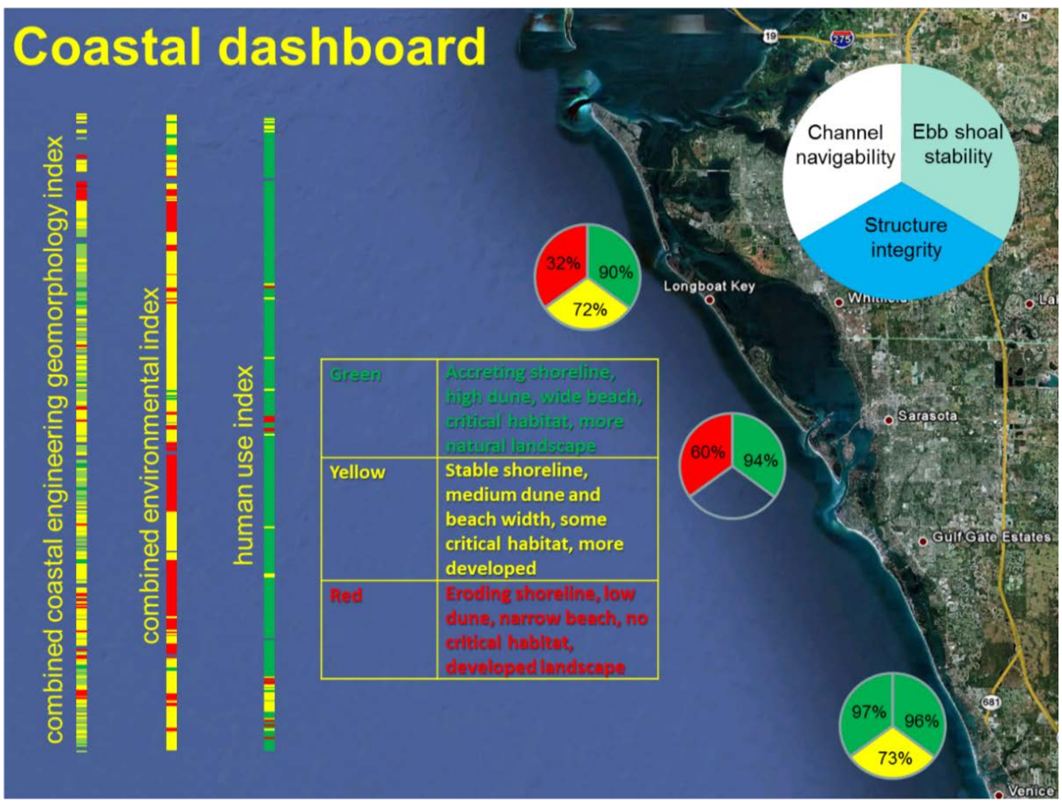

Figure 7.7.1. Coastal dashboard of demonstration area from Tampa Bay south to Venice Inlet, Florida. The set of stoplight indicators generated from extracted geomorpological, environmental, and infrastructure metrics and parameters, give an immediate illustration of coastal conditions. Figure adapted from Wozencraft et al., 2018.

Airborne coastal mapping data are also uniquely available to support studies of coastal resilince, which require data and information about many different aspects of the coastal zone. Features extracted from

eCommons (2019) https://doi.org/10.7298/tbxj-3067

airborne coastal mapping data can be used to define an index of coastal resilience. *Figure 7.7.2* shows a conceptual model where features extracted from airborne coastal mapping data are used in a multi-criteria index that notionally defines coastal resilience. The resilience index will soon be validated against results from the last hurricane season. The time series of coastal mapping data available before and after storms from 2004 to present has yet to be analyzed in terms of what we can learn about impacts and recovery from coastal storms, and how that can inform planning for future events and engineering coastal resilience.

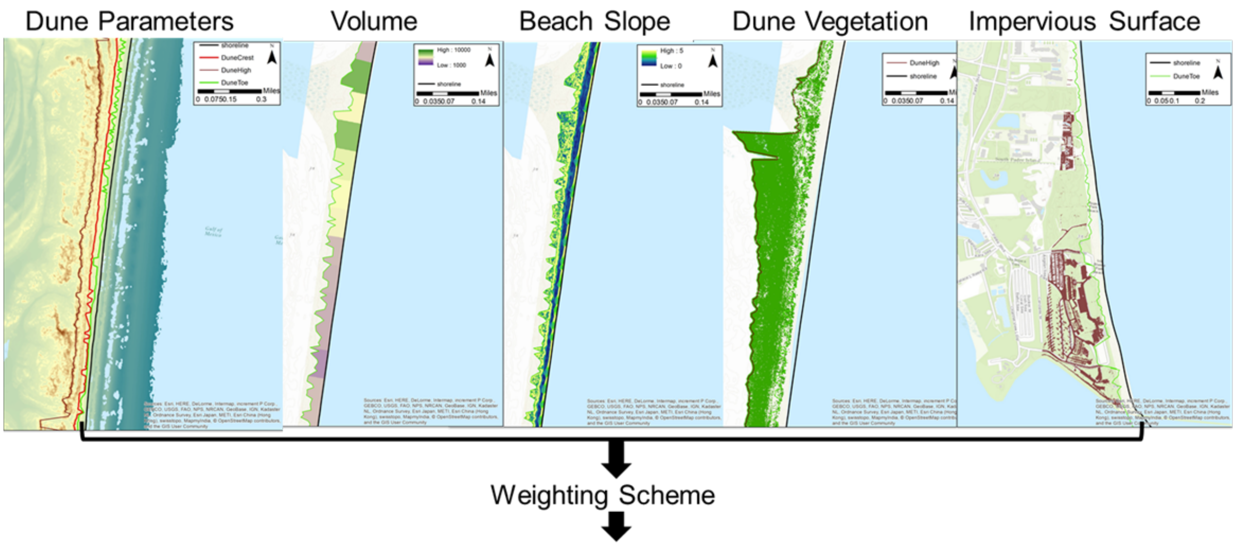

$$
\begin{aligned}
Resiliency = 0.7\Big\{ & \left(0.7\frac{Dune\ Peak}{Max\ Dune\ Peak}\right) + 0.2\left(\frac{Barrier\ Island\ CS\ Volume}{Max\ B.I.C.S.Volume}\right) \\
& + 0.1\left(\frac{Max\ Shoreline\ Erosion - Shoreline\ Erosion}{Max\ Shoreline\ Erosion}\right)\Big\} && \textbf{Tier 1} \\
& + 0.2\Big\{0.45\left(\frac{Barrier\ Island\ Width}{Max\ B.I.Width}\right) + 0.1\left(\frac{Beach\ Width}{Max\ Beach\ Width}\right) \\
& + 0.04\left(\frac{Slope\ of\ Beach}{Max\ Slope\ of\ Beach}\right) + 0.03\left(\frac{Slope\ to\ Depth\ of\ Closure}{Max\ Slope\ to\ D.of\ Closure}\right) \\
& + 0.3\left(\frac{Impervious\ Area}{Max\ Impervious\ Area}\right) + 0.2\left(\frac{Dune\ Veg.Coverage}{Max\ Dune\ Veg.Coverage}\right) && \textbf{Tier 2} \\
& + 0.05\left(\frac{Height\ of\ Veg.\ above\ Ground}{Max\ Height\ Veg.above\ Ground}\right) + 0.05\left(\frac{Bay\ Volume}{Max\ Bay\ Volume}\right) \\
& + 0.05\left(\frac{Max.Relative\ Sea\ Level\ Change - Rel.\ Sea\ Level\ Change}{Max.Rel.\ Sea\ Level\ Change}\right)\Big\} \\
& + 0.1\Big\{0.15\left(\frac{Tidal\ Prism}{Max\ Tidal\ Prism}\right) + 0.6\left(\frac{Max\ Breach\ History - Breach\ Hist.}{Max\ Breach\ Hist.}\right) && \textbf{Tier 3} \\
& + 0.25\left(\frac{Dune\ Toe}{Max\ Dune\ Toe}\right)\Big\}
\end{aligned}
$$

Figure 7.7.2. Features extracted from airborne coastal mapping data and proposed weighting scheme for multi-criteria resiliency index

We have only begun to scratch the surface of what can be learned from these valuable datasets. New systems with expanded capabilities and deployment from new platforms will enable even more exciting work in the realm of airborne coastal mapping applications.

eCommons (2019) https://doi.org/10.7298/tbxj-3067

7.8 References

Aitken, Jennifer, Vinod Ramnath, Viktor I. Feygels, Abhinav Mathur, Minsu Kim, Joong Yong Park, and Grady H. Tuell. 2010. "Prelude to CZMIL: Seafloor Imaging and Classification Results Achieved with CHARTS and the Rapid Environmental Assessment (REA) Processor." In *Algorithms and Technologies for Multispectral, Hyperspectral, and Ultraspectral Imagery XVI, April 5, 2010 - April 8*, 7695:The Society of Photo-Optical Instrumentation Engin. Optech International, 7225 Stennis Airport Road, Kiln, MS 39556, United States: SPIE. https://doi.org/10.1117/12.851915.

Aslaksen, M.L., K. Waters, Jennifer M. Wozencraft, Christopher L. Macon, John Brock, C. Wayne Right, and Christopher E. Parrish. 2012. "Coastal Applications." In *Manual of Airborne Topographic Lidar*, edited by M.S. Renslow.

Baird, W.F. & Assoc. 2002. "Regional Sediment Management (RSM), Sediment Budget for St. Joseph, MI to Michigan City." In *USACE Report Prepared for Detroit District USACE*.

Bocamazo, L.M., W.G. Grosskopf, and F.S. Buonuiato. 2011. "Beach Nourishment, Shoreline Change, and Dune Growth at Westhampton Beach, New York, 1996-2009." In *Symposium to Honor Dr. Nicholas C. Kraus*, edited by T.M. Roberts, J.D. Rosati, and P. Wang, Proceeding:181–91.

Chust, Guillem, Maitane Grande, Ibon Galparsoro, Adolfo Uriarte, and Angel Borja. 2010. "Capabilities of the Bathymetric Hawk Eye LiDAR for Coastal Habitat Mapping: A Case Study within a Basque Estuary." *Estuarine Coastal and Shelf Science* 89 (3): 200–213. https://doi.org/10.1016/j.ecss.2010.07.002.

Collin, Antoine, Bernard F. Long, and Phillippe Archambault. 2011. "Benthic Classifications Using Bathymetric LIDAR Waveforms and Integration of Local Spatial Statistics and Textural Features." *Journal of Coastal Research* 27 (February): 86–98. https://doi.org/10.2112/SI_62_9.

Cottin, Antoine G., Donald L. Forbes, and Bernard F. Long. 2009. "Shallow Seabed Mapping and Classification Using Waveform Analysis and Bathymetry from SHOALS Lidar Data." *Canadian Journal of Remote Sensing* 35 (5): 422–34.

Dunkin, Lauren M., and John McCormick. 2011. "Monitoring Shore Protection Projects along the Florida Panhandle Using Three-Dimensional Spatial Data." In . Proceedings. San Diego, CA: ASCE. https://doi.org/10.1061/41190(422)62.

Dunkin, Lauren, Molly Reif, Safra Altman, and Todd Swannack. 2016. "A Spatially Explicit, Multi-Criteria Decision Support Model for Loggerhead Sea Turtle Nesting Habitat Suitability: A Remote Sensing-Based Approach." *Remote Sensing* 8 (7): 573. https://doi.org/10.3390/rs8070573.

Eisemann, Eve R, Davin J Wallace, Maarten C Buijsman, and Troy Pierce. 2018. "Response of a Vulnerable Barrier Island to Multi-Year Storm Impacts: LiDAR-Data-Inferred Morphodynamic Changes on Ship Island, Mississippi, USA." *Geomorphology* 313: 58–71. https://doi.org/https://doi.org/10.1016/j.geomorph.2018.04.001.

Gares, Paul A, Yong Wang, and Stephen A White. 2006. "Using LIDAR to Monitor a Beach Nourishment Project at Wrightsville Beach, North Carolina, USA." *Journal of Coastal Research* 22 (5): 1206–19. http://www.jstor.org.proxy.library.cornell.edu/stable/4300387.

Graham, T., K. Smith, J. Spittal, and G. R. West. 1999. "Improving the Efficiency, Safety and Economy of the New Zealand National Nautical Charting Program through the Integrated Use of the SHOALS System in a Multi-Sensor Survey." In *Proc. U.S. Hydrographic Conference*, 11 pp. Mobile, AL.

Hapke, C.J., S. Malone, and M. Kratzmann. 2009. "National Assessment of Historical Shoreline Change: A Pilot Study of Historical Coastal Bluff Retreat in the Great Lakes, Erie, Pennsylvania." In *USGS Open-File Report 2009-1042*.

Hapke, C.J., and D. Reid. 2007. "National Assessment of Shoreline Change Part 4: Historical Coastal Cliff Retreat along the California Coast." In *USGS Open File Report 20047-1133*.

Irish, Jennifer L., and W. Jeff Lillycrop. 1997. "Monitoring New Pass, Florida, with High Density Lidar Bathymetry." *Journal of Coastal Research* 13 (4): 1130–40. https://doi.org/10.2307/4298721.

———. 1999. “Scanning Laser Mapping of the Coastal Zone: The SHOALS System.” *ISPRS Journal of Photogrammetry and Remote Sensing* 54 (2–3): 123–29. https://doi.org/10.1016/S0924-2716(99)00003-9.

Irish, Jennifer L., W. Jeff Lillycrop, and Larry E. Parson. 1997. “Accuracy of Sand Volumes as a Function of Survey Density.” In *Part 1 (of 4), September 2, 1996 - September 6*, 3:3736–49. Proceedings of the 1996 25th International Conference on Coastal Engineering. US Army Engineer Waterways, Experiment Station, Vicksburg, United States: ASCE.

Irish, Jennifer L., J. E. Thomas, Larry E. Parson, and W. Jeff Lillycrop. 1996. “Monitoring Storm Response with High Density Lidar Bathymetry: The Effects of Hurricane Opal on Florida’s Panhandle.” In *Proc. 2nd Int. Airborne Remote Sensing Conf.*, III:723–32. San Francisco, CA.

Irish, Jennifer L., and T. E. White. 1998. “Coastal Engineering Applications of High-Resolution Lidar Bathymetry.” *Coastal Engineering* 35 (1–2): 47–71. https://doi.org/10.1016/S0378-3839(98)00022-2.

Kim, Minsu, Joong Yong Park, and Grady H. Tuell. 2010. “A Constrained Optimization Technique for Estimating Environmental Parameters from CZMIL Hyperspectral and Lidar Data.” In *SPIE 7695: Algorithms and Technologies for Multispectral, Hyperspectral, and Ultraspectral Imagery XVI, April 5-8, 2010*. Vol. 7695. SPIE. https://doi.org/10.1117/12.851989.

Lillycrop, W. Jeff, and John R. Banic. 1992. “Advancements in the US Army Corps of Engineers Hydrographic Survey Capabilities: The SHOALS System.” *Marine Geodesy*, Mar. Geod. (USA), 15 (2–3): 177–85. https://doi.org/10.1080/01490419209388053.

Lillycrop, W. Jeff, Robert W. Pope, and Geraint R. West. 2000. “Rapid Environmental Assessment with Lidar.” *GPS World: News and Applications of the Global Positioning System*, November 2000.

List, Jeffrey H., Amy S. Farris, and Charlene Sullivan. 2006. “Reversing Storm Hotspots on Sandy Beaches: Spatial and Temporal Characteristics.” *Marine Geology* 226 (3–4): 261–79. https://doi.org/10.1016/j.margeo.2005.10.003.

Liu, Jung-Kung, Rongxing Li, Sagar Deshpande, Xutong Niu, and Tian-Yuan Shih. 2009. “Estimation of Blufflines Using Topographic Lidar Data and Orthoimages.” *Photogrammetric Engineering & Remote Sensing* 75 (1): 69–79. https://www.asprs.org/wp-content/uploads/pers/2009journal/january/2009_jan_57-68.pdf.

McClung, J. K. 1998. “High Density Lidar Data: A Monitoring Tool for East Pass Florida.” In *Proc. 5th Int’l Conf. on Remote Sensing for Marine and Coastal Environmnents*, I:75–82. San Diego, CA.

McNinch, Jesse E. 2004. “Geologic Control in the Nearshore: Shore-Oblique Sandbars and Shoreline Erosional Hotspots, Mid-Atlantic Bight, USA.” *Marine Geology* 211 (1–2): 121–41. https://doi.org/10.1016/j.margeo.2004.07.006.

Mohr, M. C., J. Pope, and J. K. McClung. 1999. “Coastal Response to a Detached Breakwater System; Presque Isle, Pennsylvania, USA.” In *Proc. 4th International Symposium on Coastal Engineering and Science of Coastal Sediment Processes*, 3:2010–25. Long Island, NY: American Society of Civil Engineers.

Nayegandhi, Amar, John C. Brock, C. Wayne Wright, and Michael J. O’Connell. 2006. “Evaluating A Small Footprint, Waveform-Resolving Lidar Over Coastal Vegetation Communities.” *Photogrammetric Engineering and Remote Sensing* 72 (12): 1407–17. https://doi.org/0099-1112.

Palaseanu-Lovejoy, Monica, Jeffrey J. Danielson, Cindy Thatcher, Amy C. Foxgrover, Patrick L. Barnard, John C. Brock, and Adam Young. 2016. “Automatic Delineation of Seacliff Limits Using Lidar-Derived High-Resolution DEMs in Southern California.” *Journal of Coastal Research* SI (76): 162–73. https://doi.org/10.2112/SI76-014.

Palaseanu-Lovejoy, Monica, Amar Nayegandhi, John Brock, Robert Woodman, and C Wayne Wright. 2009. “Evaluation of Airborne Lidar Data to Predict Vegetation Presence/Absence.” *Journal of Coastal Research* 25 (6): 83–97. http://www.jstor.org.proxy.library.cornell.edu/stable/25737455.

Pastol, Yves. 2011. “Use of Airborne LIDAR Bathymetry for Coastal Hydrographic Surveying: The French Experience.” *Journal of Coastal Research* 62 (March): 6–18. https://doi.org/10.2112/SI_62_2.

Pittman, Simon J., Bryan M. Costa, and Timothy A. Battista. 2009. “Using Lidar Bathymetry and Boosted Regression Trees to Predict the Diversity and Abundance of Fish and Corals.” *Journal of Coastal Research* 25 (6): 27–38. https://doi.org/10.2112/SI53-004.1.

Pope, Robert W., B. A. Reed, Geraint R. West, and W. Jeff Lillycrop. 1997. “Use of an Airborne Laser Depth Sounding System in a Complex Shallow-Water Environment.” In *Proc. 15th Int’l Hydro Conference*, 10 pgs. Monaco.

Reif, Molly K., Christopher L. Macon, and Jennifer M. Wozencraft. 2011. “Post-Katrina Land-Cover, Elevation, and Volume Change Assessment along the South Shore of Lake Pontchartrain, Louisiana, USA.” *Journal of Coastal Research*, 30–39. https://doi.org/10.2112/SI_62_4.

Reif, Molly K., C. Piercy, J. Jarvis, B. Sabol, Christopher L. Macon, R. Lloyd, H. Colarusso, Heidi M. Dierssen, and Jennifer Aitken. 2012. *A Case Study of Ground Truth Sampling to Support Sensing Research and Development: Submersed Aquatic Vegetation Species Discrimination Using an Airborne Hyperspectral/Lidar System*. DOER Technical Notes Collection. Vicksburg, MS: U.S. Army Engineer Research and Development Center.

Reif, Molly K., and T. M. Swannack. 2014. “Development of Landscape Metrics to Support Process-Driven Ecological Modeling.” ERDC/EL TR-14-6. Vicksburg, MS.

Reif, Molly K, Jennifer M Wozencraft, Lauren M Dunkin, Charlene S Sylvester, and Christopher L Macon. 2013. “A Review of U.S. Army Corps of Engineers Airborne Coastal Mapping in the Great Lakes.” *Journal of Great Lakes Research* 39: 194–204. https://doi.org/https://doi.org/10.1016/j.jglr.2012.11.002.

Robertson, William, V, Dean Whitman, Keqi Zhang, and Stephen P Leatherman. 2004. “Mapping Shoreline Position Using Airborne Laser Altimetry.” *Journal of Coastal Research* 20 (3): 884–92. http://www.jstor.org.proxy.library.cornell.edu/stable/4299347.

Robertson, Quin, Lauren M. Dunkin, Zhifei Dong, Jennifer M. Wozencraft, and Keqi Zhang. 2018. “Florida and US East Coast Beach Change Metrics Derived from LiDAR Data Utilizing ArcGIS Python Based Tools.” In *Beach Management Tools - Concepts, Methodologies and Case Studies*, 239–58. Coastal Research Library. Springer, Cham.

Rosati, Julie Dean. 2005. “Concepts in Sediment Budgets.” *Journal of Coastal Research* 212 (March): 307–22. https://doi.org/10.2112/02-475A.1.

Sallenger, Asbury H., Hilary F. Stockdon, Laura A. Fauver, Mark Hansen, David Thompson, C. Wayne Wright, and W. Jeff Lillycrop. 2006. “Hurricanes 2004: An Overview of Their Characteristics and Coastal Change.” *Estuaries and Coasts; Port Republic* 29 (6): 880–88. https://doi.org/http://dx.doi.org.proxy.library.cornell.edu/10.1007/BF02798647.

Sallenger, Asbury H., C. Wayne Wright, and W. Jeff Lillycrop. 2005. “Coastal Impacts of the 2004 Hurricanes Measured with Airborne Lidar; Initial Results.” *Shore and Beach* 73 (2&3): 10–14.

Schupp, Courtney A., Jesse E. McNinch, and Jeffrey H. List. 2006. “Nearshore Shore-Oblique Bars, Gravel Outcrops, and Their Correlation to Shoreline Change.” *Marine Geology* 233 (1–4): 63–79. https://doi.org/10.1016/J.MARGEO.2006.08.007.

Stauble, Donald K. 2003. “The Use of Shoreline Change Mapping in Coastal Engineering Project Assessment.” *Journal of Coastal Research*, 178–206. http://www.jstor.org/stable/25736606.

Stockdon, Hilary F., Jr. Sallenger, Asbury H., Jeffrey H. List, and Rob A. Holman. 2002. “Estimation of Shoreline Position and Change Using Airborne Topographic Lidar Data.” *Journal of Coastal Research* 18 (3): 502–13. http://www.jstor.org.proxy.library.cornell.edu/stable/4299097.

Stockdon, Hilary F, Kara S Doran, and Asbury H Sallenger. 2009. “Extraction of Lidar-Based Dune-Crest Elevations for Use in Examining the Vulnerability of Beaches to Inundation During Hurricanes.”

Journal of Coastal Research 25 (6 Supplement. Special Issue No 53): 59–65. http://www.jstor.org.proxy.library.cornell.edu/stable/25737452.

Thieler, E.R., E.A. Himmelstoss, J.L. Zichichi, and A. Ergul. 2009. "The Digital Shoreline Analysis System (DSAS) Version 4.0, an ArcGIS Extension for Calculating Shoreline Change URL: ." In *U.S. Geological Survey Open-File Report 2008-1278*. http://pubs.usgs.gov/of/2008/1278/.

Walker, Brian K., Bernhard Riegl, and Richard E. Dodge. 2008. "Mapping Coral Reef Habitats in Southeast Florida Using a Combined Technique Approach." *Journal of Coastal Research* 24 (5): 1138–50. https://doi.org/10.2112/06-0809.1.

Wallace, Davin J., John B. Anderson, and Antonio B. Rodriguez. 2009. "Natural versus Anthropogenic Mechanisms of Erosion along the Upper Texas Coast." In *America's Most Vulnerable Coastal Communities*. Geological Society of America. https://doi.org/10.1130/2009.2460(10).

Wang, Chau-Chang, and Dajun Tang. 2012. "Application of Underwater Laser Scanning for Seafloor Shell Fragments Characterization." *Journal of Marine Science and Technology-Taiwan* 20 (1): 95–102.

Wang, Chi-Kuei, and William D. Philpot. 2007. "Using Airborne Bathymetric Lidar to Detect Bottom Type Variation in Shallow Waters." *Remote Sensing of Environment* 106 (1): 123–35. https://doi.org/10.1016/j.rse.2006.08.003.

Weber, Kathryn M., Jeffrey H. List, and Karen L.M. Morgan. 2005. "An Operational Mean High Water Datum for Determination of Shoreline Position from Topographic Lidar Data." *Open-File Report*. https://doi.org/10.3133/OFR20051027.

West, Geraint R. 2001. "In Deeper Waters." *POB*, March 2001.

West, Geraint R., and W. Jeff Lillycrop. 1999. "Feature Detection and Classification with Airborne Lidar - Practical Experience." In *Proc. Shallow Survey 99*. Sydney, Australia.

West, Geraint R., and C. E. Wiggins. 2000. "Airborne Mapping Sheds Light on Hawaiian Coasts and Harbors." *Earth Observation Magazine (EOM)*, 2000.

White, Stephen A. 2007. "Utilization of Lidar and NOAA's Vertical Datum Transformation Tool (VDatum) for Shoreline Delineation." In *Marine Technology Society/IEEE Oceans Conference*, 1–6. Vancouver, BC: IEEE. https://doi.org/10.1109/OCEANS.2007.4449147.

White, Stephen A., Christopher E. Parrish, Brian R. Calder, Shachak Pe'eri, and Yuri Rzhanov. 2011. "LIDAR-Derived National Shoreline: Empirical and Stochastic Uncertainty Analyses." *Journal of Coastal Research*, no. 62 (Special Issue): 62–74. https://doi.org/10.2112/SI_62_7.

Wozencraft, Jennifer M. 2001. "Sand Volumes and Transport Pathways for Gulf of Mexico Regional Sediment Management." In *Coastal Dynamics '01*, 693–702. Proceedings. Bergen, Norway: ASCE. https://doi.org/10.1061/40566(260)71.

———. 2013. "Using LiDAR to Assess Storm Damage Caused by Hurricane Sandy." *LiDAR Magazine*, March 2013.

Wozencraft, Jennifer M., Lauren M. Dunkin, Molly K. Reif, and E. Eisemann. 2018. "A Spatial Index Approach to Coastal Monitoring: A Florida Case Study." Edited by R Almar, L P Almeida, Viet N Trung, and Sall. *Journal of Coastal Research*, no. 81 (Special Issue): Tropical, Coastal, and Estutarine Dynamics: 67–75. https://www-jstor-org.proxy.library.cornell.edu/stable/26552353.

Wozencraft, Jennifer M., and Jennifer L. Irish. 2000. "Airborne Lidar Surveys and Regional Sediment Management." In *Proc. 20th EARSeL Symposium*, 11 pgs. Dresden, Germany: European Association of Remote Sensing Laboratories EARSeL.

Wozencraft, Jennifer M., and W. Jeff Lillycrop. 2006. "JALBTCX Coastal Mapping for the USACE." *The International Hydrographic Review* 7 (2): 28–37. https://journals.lib.unb.ca/index.php/ihr/article/view/20763.

Wozencraft, Jennifer M., and David Millar. 2005. "Airborne Lidar and Integrated Technologies for Coastal Mapping and Nautical Charting." *Marine Technology Society Journal* 39 (3): 27–35.

https://doi.org/10.4031/002533205787442440.

Wozencraft, Jennifer M., and Joong Yong Park. 2013. "Integrated LiDAR and Hyperspectral." In *Coral Reef Remote Sensing*, 1st ed., 175–91. Dordrecht: Springer Netherlands. https://doi.org/10.1007/978-90-481-9292-2_7.

Xhardé, Régis, Bernard F. Long, and Donald L. Forbes. 2011. "Short-Term Beach and Shoreface Evolution on a Cuspate Foreland Observed with Airborne Topographic and Bathymetric LIDAR." *Journal of Coastal Research*, no. Special Issue No 62: Applied Lidar Techniques (March): 50–61. https://doi.org/10.2112/SI_62_6.

Yamamoto, Kristina H., Rebecca L. Powell, Sharolyn Anderson, and Paul C. Sutton. 2012. "Using LiDAR to Quantify Topographic and Bathymetric Details for Sea Turtle Nesting Beaches in Florida." *Remote Sensing of Environment* 125 (October): 125–33. https://doi.org/10.1016/j.rse.2012.07.016.

Young, Adam P, and Scott A Ashford. 2006. "Application of Airborne LIDAR for Seacliff Volumetric Change and Beach-Sediment Budget Contributions." *Journal of Coastal Research* 22 (2): 307–18. http://www.jstor.org.proxy.library.cornell.edu/stable/4300288.

Zawada, David G., and John C. Brock. 2009. "A Multiscale Analysis of Coral Reef Topographic Complexity Using Lidar-Derived Bathymetry." *Journal of Coastal Research* 25 (6): 6–15. https://doi.org/10.2112/SI53-002.1.

Zhang, Keqi, Dean Whitman, Stephen Leatherman, and William V. Robertson. 2005. "Quantification of Beach Changes Caused by Hurricane Floyd Along Florida's Atlantic Coast Using Airborne Laser Surveys." *Journal of Coastal Research* 211 (1): 123–34. https://doi.org/10.2112/02057.1.